

Suppressing coherence effects in quantum-measurement-based engines

Zhiyuan Lin,^{1,*} Shanhe Su,^{1,*†} Jingyi Chen,¹ Jincan Chen ^{1,‡} and Jonas F. G. Santos²

¹*Department of Physics, Xiamen University, Xiamen 361005, People's Republic of China*

²*Centro de Ciências Naturais e Humanas, Universidade Federal do ABC, Avenida dos Estados 5001, 09210-580 Santo André, São Paulo, Brazil*



(Received 7 September 2021; accepted 9 December 2021; published 22 December 2021)

Recent advances in the study of thermodynamics of microscopic processes have driven the search for new developments in energy converters utilizing quantum effects. Here we propose a modified Otto cycle to design an engine fueled by quantum projective measurements. Standard quantum thermal machines operating in a finite-time regime with a driven Hamiltonian that does not commute at different times have their performance decreased by the presence of coherence, which is associated with a larger entropy production and irreversibility degree. However, we show that replacing the standard hot thermal reservoir by a projective measurement operation with a general basis in the Bloch sphere and controlling the basis angles suitably could improve the performance of the quantum engine as well as decrease the entropy change during the measurement process. Our results follow a generalization of quantum thermal machine models where the fuel comes from general sources beyond the standard thermal reservoir.

DOI: [10.1103/PhysRevA.104.062210](https://doi.org/10.1103/PhysRevA.104.062210)

I. INTRODUCTION

The current development of new devices based on quantum effects has shown that a well-formulated understanding of quantum thermodynamics is required [1–4]. Recent progress in quantum fluctuation relations [5–7], thermodynamic uncertainty relations [8–10], and the study of quantum protocols involving nonequilibrium thermal baths [11–14], the strong-coupling regime [15,16], and non-Markovian effects [17,18] must be highlighted.

Encompassing the above-mentioned results, the study of quantum thermal machines (QTMs) is useful to investigate how specific driving protocols or nonclassical baths impact the performance of thermodynamic cycles. In this direction, it is well known that coherence in the energy basis of the working substance leads to the increase of entropy production along the cycle [19–22]. The theoretical design of QTMs employing non-Markovian thermal baths [23–26], finite-size environments [27], and squeezed thermal baths [28–30] is another interesting aspect that has been addressed. For a QTM operating in a finite-time Otto cycle, reaching the limit efficiency with a nonzero extracted power is motivated by realistic applications. From an experimental point of view, realizations of a single-spin Otto cycle have been performed in nuclear magnetic resonance (NMR) [31] and in an ensemble of nitrogen-vacancy centers in diamond [32], both revealing the generation of coherence in the energy basis of the working substance. Also, an experimental verification of the fluctuation relation for work and heat in a quantum engine was reported in Ref. [33], showing how correlations between

work and heat affect the performance of a finite-time quantum engine.

Apart from the standard cycles, a more general type of QTM was proposed by Szilard [34] that differs from the former models in the sense that energy is extracted from a single heat bath by using a feedback mechanism well known as Maxwell's demon [35,36]. This evidences that information can effectively work as the fuel [37,38]. In order to have information flowing into the system, we necessarily need to measure the system by employing a specific protocol. Since a measurement performed on a quantum system generally alters its state, recent advances have proposed measurement-driven engines, in which the measurement protocol itself provides the fuel and allows for work extraction. Yi *et al.* [39] and Ding *et al.* [40] designed a single-temperature engine consisting of isentropic compression, energy input at measurement, isentropic expansion, and rejection of heat at thermalization. Elouard *et al.* introduced a new protocol of Maxwell's demon engines, where work is directly extracted from the measurement instead of a hot reservoir [36,41]. Brandner *et al.* obtained the efficiency of information to work conversion by considering a system repeatedly coupled to a bath or to a coherent laser pulse conditioned on the outcome of a projective measurement [42]. Jordan *et al.* provided a complete interpretation of the recent achievements for developing quantum measurement engines [43]. Measurement-driven machines were extended to composite working substances as well. For a two-stroke two-qubit cooler, the singlet-triplet basis maximizes the energy extraction [44]. An alternate scheme introduced a two-qubit engine powered by entanglement and local measurements [45]. For standard projective measurements, the system state is entirely collapsed to a specific eigenstate. There is also a special activity concerning the so-called weak measurement [46–50], whose system state is only partially perturbed [49–55].

*These authors contributed equally to this work.

†sushanhe@xmu.edu.cn

‡jcchen@xmu.edu.cn

A natural question that arises in thermodynamic cycles is how to reveal the role played by quantum measurements in the energy conversion and the possibility to suitably engender quantum measurements to enhance the performance of QTMs. Replacing the standard hot reservoir by a quantum measurement protocol provides a new degree of freedom for the cycle which depends essentially on the measurement basis. Thus, from the point of view of the friction induced by transitions between the eigenstates of the working substance [56–58], quantum projective measurements with a suitable basis on the Bloch sphere could be understood as a kind of quantum lubricant if it attenuates the degradation effect due to the presence of coherence.

In this work we are interested in addressing how quantum fluctuations associated with finite-time driven unitary processes and quantum measurements affect the performance of a quantum engine. For this purpose, we consider a modified version of the quantum Otto cycle where the standard hot thermal reservoir is replaced by a quantum projective measurement, providing a different mechanism to fuel the cycle. In order to understand the role played by two kinds of quantum fluctuations, we present explicitly expressions for the thermodynamic quantities characterizing the engine and its performance. Considering a numerical simulation with parameters employed in the NMR setup [59], we show that by having sufficient control over the choice of the measurement basis, it is possible to enhance the work extraction and then the performance of the quantum engine. Since the irreversibility of the cycle is associated with the increase of entropy, we also show that the maximum values of efficiency and extracted work are reached very close to the minimum value of entropy change during the measurement protocol.

II. CYCLE OF THE ENGINE BASED ON QUANTUM MEASUREMENT

The quantum measurement engine employs a particle of spin $\frac{1}{2}$ (single qubit) as the working substance. To complete one operating cycle, the engine goes through four strokes, including two unitary transformation processes, a quantum measurement process, and a thermalization process, as sketched in Fig. 1. The working substance is initially prepared in thermal equilibrium with a heat bath at positive inverse temperature β such that its state at time $t = 0$ is given by $\rho_1 = e^{-\beta H_1}/Z_1$ [60,61], where $H_1 = \frac{\hbar\omega}{2}\sigma_z$ is the initial Hamiltonian, $Z_1 = \text{Tr}(e^{-\beta H_1})$ is the partition function, \hbar is the reduced Planck constant, ω denotes the resonance frequency, and σ_i ($i = x, y, z$) are the Pauli matrices.

During the unitary transformation at stage I, a time-modulated radio-frequency field generates a time-dependent Hamiltonian $H_I(t) = \frac{\hbar\omega}{2}(\cos\frac{\pi t}{2\tau}\sigma_z + \sin\frac{\pi t}{2\tau}\sigma_x)$, which clearly does not commute at different times, implying the generation of coherence in the energy basis of the working substance [19]. At $t = \tau$, the working substance changes into state $\rho_2 = U_{\tau,0}\rho_1 U_{\tau,0}^\dagger$, with $U_{\tau,0} = \mathcal{T} \exp[-\frac{i}{\hbar} \int_0^\tau H_I(t) dt]$ the time-evolution operator and \mathcal{T} the time-ordering operator. The work performed on the spin $\langle W_1 \rangle = \text{Tr}(\rho_2 H_2 - \rho_1 H_1)$, where $H_2 = \frac{\hbar\omega}{2}\sigma_x$ represents the final Hamiltonian. After the quantum measurement at stage II, the state of the spin is updated to $\rho_3 = \sum_k \pi_k \rho_2 \pi_k$ [62,63], where $\pi_k = |\chi_k\rangle\langle\chi_k|$ defines

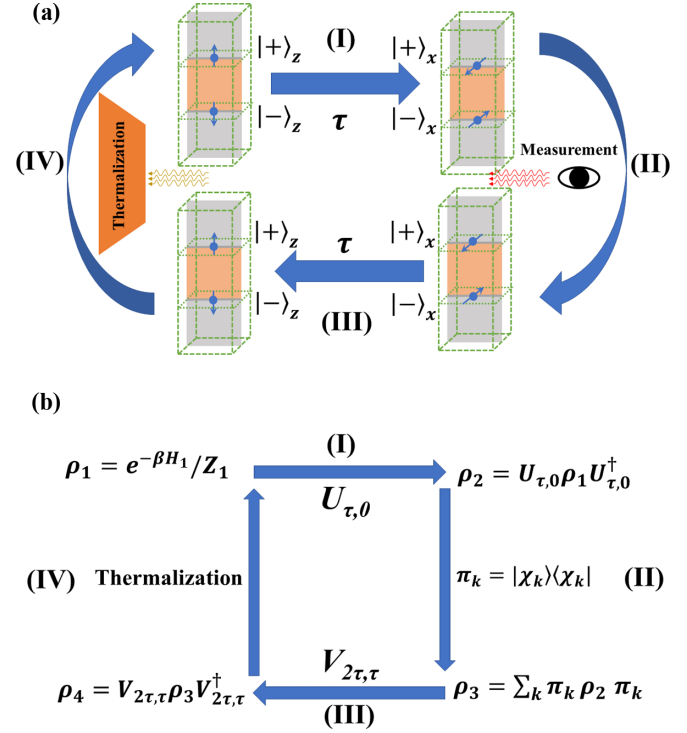


FIG. 1. Illustration of the engine based on quantum measurement. (a) The working substance starts in thermal equilibrium with the heat bath. The first stroke is a unitary transformation process mediated by a time-dependent Hamiltonian. In the second stroke, an instantaneous projective measurement is performed on the working substance, projecting the single qubit onto the basis $\{|\chi_1\rangle, |\chi_2\rangle\}$. The third stroke is again a unitary evolution using a time-dependent Hamiltonian. In the fourth stroke, the working substance relaxes to the initial thermal equilibrium state. (b) Evolution of the density matrix during the cycle

the orthogonal projector associated with the measurement bases $|\chi_1\rangle = e^{-i\varphi} \sin\frac{\alpha}{2}|\uparrow\rangle - \cos\frac{\alpha}{2}|\downarrow\rangle$ and $|\chi_2\rangle = \cos\frac{\alpha}{2}|\uparrow\rangle + e^{i\varphi} \sin\frac{\alpha}{2}|\downarrow\rangle$. In the Bloch sphere representation, α and φ are the colatitude with respect to the z axis and the longitude with respect to the x axis, respectively. The total fuel energy provided by quantum measurement $\langle Q_M \rangle = \text{Tr}[H_2(\rho_3 - \rho_2)]$. During the unitary transformation at stage III, the driving Hamiltonian $H_{II}(t) = H_I(2\tau - t)$, with $t \in [\tau, 2\tau]$. The final state of this stroke $\rho_4 = V_{2\tau,\tau}\rho_3 V_{2\tau,\tau}^\dagger$, where the unitary operator $V_{2\tau,\tau} = \mathcal{T} \exp[-\frac{i}{\hbar} \int_\tau^{2\tau} H_{II}(t) dt]$. The work performed by the external field $\langle W_2 \rangle = \text{Tr}(\rho_4 H_1 - \rho_3 H_2)$. The spin returns to the initial Gibbs state ρ_1 for a thermalization process at stage IV. The heat $\langle Q_T \rangle$ flowing into the spin from the bath $\langle Q_T \rangle = \text{Tr}(H_1 \rho_1 - H_1 \rho_4)$.

A more detailed description of the cycle of the quantum measurement engine is given in [64]. Note that the four-step cycle was introduced in Ref. [39]. Following the proposal in Ref. [43], we consider the situation where the quantum adiabatic process is replaced by the unitary transformation and the measurement basis can be optimized. One is capable of proving that $\langle Q_T \rangle$ is always negative, meaning that energy is actually flowing from the working substance into the heat bath (see [64]). It is impossible for the thermodynamic cycle

to convert the heat from a single source into work without any other effect, satisfying Kelvin’s statement of the second law of thermodynamics.

III. ROLES OF TRANSITION PROBABILITIES IN THE PERFORMANCE OF THE ENGINE

The net work done by the external agent is

$$\begin{aligned} \langle W \rangle &= \langle W_1 \rangle + \langle W_2 \rangle \\ &= \hbar\omega[\xi - (\delta - \gamma)(1 - 2\zeta)] \tanh\left(\frac{\beta\hbar\omega}{2}\right), \end{aligned} \quad (1)$$

where $\zeta = |\langle\chi_2|U_{\tau,0}|-\rangle_z|^2$ is the transition probability between the basis state $|\chi_2\rangle$ of measurement and the ground eigenstate $|-\rangle_z$ of H_1 , $\delta = |\langle\chi_2|-\rangle_x|^2$ is the transition probability between $|\chi_2\rangle$ and the ground eigenstate $|-\rangle_x$ of H_2 , $\xi = |\langle_x(+|U_{\tau,0}|-\rangle_z)|^2$ is the transition probability between the excited eigenstate $|+\rangle_x$ of H_2 and the ground eigenstate $|-\rangle_z$ of H_1 due to the unitary evolution at stage I, and $\gamma = |\langle_z(+|V_{2\tau,\tau}|\chi_1)\rangle|^2$ is the transition probability between the excited eigenstate $|+\rangle_z$ of H_1 and the basis state $|\chi_1\rangle$ of measurement due to the unitary evolution at stage III. The transition probabilities embody the influence of quantum fluctuations and satisfy the principle of microreversibility (see [64]) [65,66]. For the purpose of extracting work from the engine, we must have $\langle W \rangle < 0$. The fuel energy provided by the measurement process reads

$$\langle Q_M \rangle = \frac{\hbar\omega}{2}[(1 - 2\xi) - (1 - 2\delta)(1 - 2\zeta)] \tanh\left(\frac{\beta\hbar\omega}{2}\right). \quad (2)$$

The heat released by the working substance to the cold thermal reservoir in the thermalization process (stage IV) is written as

$$\langle Q_T \rangle = \frac{\hbar\omega}{2}[(1 - 2\gamma)(1 - 2\zeta) - 1] \tanh\left(\frac{\beta\hbar\omega}{2}\right). \quad (3)$$

Note that since $0 \leq \gamma \leq 1$ and $0 \leq \zeta \leq 1$, the inequality $\frac{1}{\gamma} \geq 2$ ensures that $\langle Q_T \rangle \leq 0$ (see [64]).

The performance of the quantum engine is dictated by the efficiency defined as $\eta = -\langle W \rangle / \langle Q_M \rangle = 1 + \langle Q_T \rangle / \langle Q_M \rangle$, where the second expression comes from the first law of thermodynamics. Using Eqs. (2) and (3), the efficiency reads

$$\eta = 1 - \frac{(1 - 2\gamma)(1 - 2\zeta) - 1}{(1 - 2\delta)(1 - 2\zeta) - (1 - 2\xi)}. \quad (4)$$

The efficiency is limited by $0 \leq \eta \leq 1$ because of the constraints $\langle Q_T \rangle \leq 0 \leq \langle Q_M \rangle$ and $|\langle Q_T \rangle| \leq |\langle Q_M \rangle|$. With the set of equations (1)–(4), all the quantum fluctuations induced by the time-dependent Hamiltonian and the measurement protocols are being taken into account and affect the performance of the engine. In particular, we will show how quantum fluctuations arising from the measurement protocols (the choice of the measurement angles) could be employed in order to suppress the degradation effect due to the coherence, thus increasing the efficiency of the cycle.

IV. NUMERICAL SIMULATION

In this section we illustrate our results with a numerical simulation with feasible parameters employed in the NMR setup. First we note that when $\alpha = \pi/2$ and $\varphi = 0$, the measurement basis commutes with the eigenstate basis of H_2 . Therefore, no energy is delivered to the working substance, resulting in zero efficiency and null extracted work. The projective quantum measurement inevitably alters the mean energy of the observed system if the measurement basis does not commute with the bare energy basis. This is the reason why quantum measurement is able to supply a continuous source of energy similar to the combustion of a fuel. Formally, the measurement basis corresponding to measuring the single qubit is a trigonometric function of the colatitude α and longitude φ . From Fig. 2 we conclude that α and φ are two crucial independent parameters used to determine the performance of the engine. The working areas of the engine are divided into two separate parts, i.e., $0 \leq \varphi \leq \pi$ and $\pi \leq \varphi \leq 2\pi$. For $0 \leq \varphi \leq \pi$, the maximum work output $(-\langle W \rangle)_{\max}$ and efficiency η_{\max} appear at different measurement directions. As depicted in Fig. 2, $-\langle W \rangle$ qualitatively peaks at $\alpha_W = 1.39$ and $\varphi_W = 2.05$, while η reaches its maximum at $\alpha_\eta = 1.45$ and $\varphi_\eta = 2.53$. To obtain the maximum attainable efficiency at a given extracted work, the optimal ranges of the extracted work and efficiency must be constrained by $\alpha_W \leq \alpha \leq \alpha_\eta$ and $\varphi_W \leq \varphi \leq \varphi_\eta$. For $\pi \leq \varphi \leq 2\pi$, the distributions of $-\langle W \rangle$ and η satisfy antisymmetry with the axis $\alpha = \pi/2$ and translational invariance, i.e., $-\langle W \rangle(\alpha, \varphi) = -\langle W \rangle(\pi - \alpha, \varphi + \pi)$ and $\eta(\alpha, \varphi) = \eta(\pi - \alpha, \varphi + \pi)$. The reason is that $-\langle W \rangle$ and η [Eqs. (1) and (4)] closely depend on the transition probabilities between the eigenstates of the instantaneous Hamiltonian and the measurement bases $|\chi_1\rangle$ and $|\chi_2\rangle$. One can find that $|\chi_1(\pi - \alpha, \varphi + \pi)\rangle = -e^{i\varphi}|\chi_2(\alpha, \varphi)\rangle$ and $|\chi_2(\pi - \alpha, \varphi + \pi)\rangle = e^{-i\varphi}|\chi_1(\alpha, \varphi)\rangle$, leading to $\zeta(\pi - \alpha, \varphi + \pi) = \zeta(\alpha, \varphi)$, $\delta(\pi - \alpha, \varphi + \pi) = \delta(\alpha, \varphi)$, and $\gamma(\pi - \alpha, \varphi + \pi) = \gamma(\alpha, \varphi)$. This directly leads to the symmetrical relationship in Figs. 2(a) and 2(b).

To understand the physics behind the enhancement of $-\langle W \rangle$ and η , we write $-\langle W \rangle$ and the quantum fuel $\langle Q_M \rangle$ in terms of the occupation probabilities, i.e.,

$$-\langle W \rangle = -\frac{\hbar\omega}{2}(\Delta p_1 - \Delta p_2 + \Delta p_3 - \Delta p_4), \quad (5)$$

$$\langle Q_M \rangle = \frac{\hbar\omega}{2}(\Delta p_2 - \Delta p_3), \quad (6)$$

where $\Delta p_1 = -\text{Tr}(\rho_1\sigma_z) = \tanh(\beta\hbar\omega/2)$, $\Delta p_2 = -\text{Tr}(\rho_2\sigma_x) = \Delta p_1(1 - 2\xi)$, $\Delta p_3 = \langle\chi_1|\rho_3|\chi_1\rangle - \langle\chi_2|\rho_3|\chi_2\rangle = \Delta p_1(1 - 2\delta)(1 - 2\zeta)$, and $\Delta p_4 = -\text{Tr}(\rho_4\sigma_z) = \Delta p_1(1 - 2\gamma)(1 - 2\zeta)$ are the difference in the occupation probabilities between the ground and excited states of each quantum state. As a result, the efficiency is simplified as

$$\eta = 1 - (\Delta p_1 - \Delta p_4) / (\Delta p_2 - \Delta p_3), \quad (7)$$

which is completely determined by the probability changes caused by the transition coefficients. For a conventional single-spin Otto cycle, the positive work condition requires the expansion and compression of the energy gap [19,31,60]. The emergence of the measurement indicates that the purpose

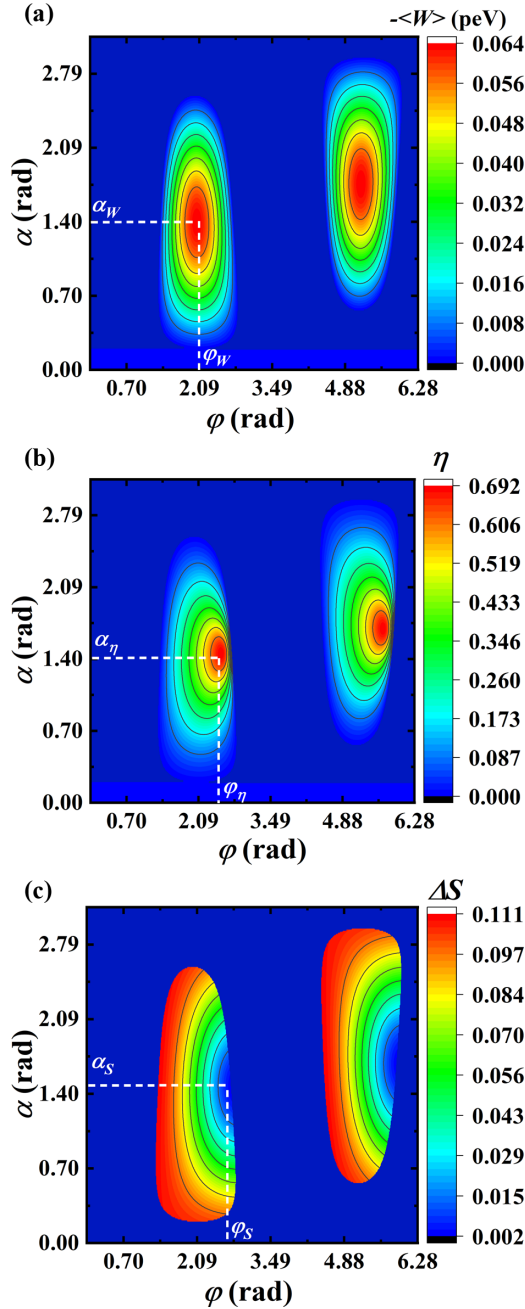


FIG. 2. Performance of the engine based on quantum measurement. (a) Extracted work $-\langle W \rangle$, (b) efficiency η , and (c) entropy change ΔS during the measurement process (stage II) varying with the colatitude α and longitude ϕ on the Bloch sphere, where $\hbar\omega = 1$ peV, $\tau = 10 \mu\text{s}$, and $\beta = 1/\hbar\omega$. These values are used unless specifically stated otherwise.

of extracting work may be achieved without changing the energy-level spacing.

Apart from the energetic exchanges in a quantum cycle, entropic quantities are inherently associated with the irreversibility of the cycle. In this sense, the entropy change of the working substance during the measurement process (state II) directly affects the performance of the engine. Figure 2(c) depicts the entropy change $\Delta S = S(\rho_3) - S(\rho_2)$ during the

measurement process, where $S(\rho_i) = -\text{Tr}(\rho_i \ln \rho_i)$ is the von Neumann entropy of a given state. The entropy change is minimum at $(\alpha_S, \phi_S) = (1.46, 2.74)$, given the parameters considered in the numerical simulation. The region of high efficiencies matches very well with the region of small entropy changes during the measurement process. This is in agreement with the prediction that decreasing the irreversibility increases the performance of quantum engines. The factors ζ , δ , and γ depend on the transitions between the measurement basis and the instantaneous energy eigenstate, resulting in quantum coherence. In Fig. 3 we observe that when $-\langle W \rangle$ and η reach their maxima, ζ , δ , and γ are large but ΔS is a relatively small value. In this sense, the measurement protocol with a suitable basis works effectively as a kind of quantum lubricant, suppressing the degradation effect due to coherence. The equalities $S(\rho_1) = S(\rho_2)$ and $S(\rho_3) = S(\rho_4)$ hold because of the invariance of von Neumann entropy under a unitary evolution. In the fourth stroke of the cycle, one can then confirm that the entropy change $S(\rho_1) - S(\rho_4)$ caused by the thermalization process is equal to $-\Delta S$.

In Fig. 3(a), $-\langle W \rangle$ and η reach their limits at $\alpha_{W'} = 1.25$ and $\alpha_{\eta} = 1.45$, respectively. However, the input energy $\langle Q_M \rangle$ is relatively small at the points of $\alpha_{W'}$ and α_{η} . We also see the behavior of the entropy change during the measurement process, evidencing that it is considerably small for high values of the efficiency. The measurement-based engine could generate a greater amount of work at low cost by optimizing the angles of the measurement basis. As the colatitude α changes, the probability changes Δp_3 and Δp_4 are the only factors that alter the useful extracted energy and the total energy input. To go a step further, the variations of Δp_3 and Δp_4 depend on the term associated with ζ , δ , and γ , as shown in Fig. 3(b). Note that the parameters ξ , Δp_1 , and Δp_2 remain constant at any given driving time and are not shown in the graph. The transition probabilities ζ , δ , and γ depending on states χ_1 and χ_2 contain all information about how quantum measurement plays an important role in thermodynamics. Figure 3(b) reveals that $1 - 2\zeta$, $1 - 2\delta$, and $1 - 2\gamma$ are convex functions of α , because their derivatives are monotonically nondecreasing. The results show that a local maximum of Δp_3 (Δp_4) exists, since the product of $1 - 2\delta(1 - 2\gamma)$ and $1 - 2\zeta$ is a concave function. It can be seen from Fig. 3(b) and Eqs. (5) and (6) that the gap between Δp_3 and Δp_4 at $\alpha_{W'}$ determines the upper bound of $-\langle W \rangle$. In addition, when Δp_3 takes the peak value, the working substance has the largest probability of being found in the ground state after the measurement and the input energy $\langle Q_M \rangle$ would be minimum.

Now we examine how the longitude ϕ of the measurement basis influences the performance. Figure 3(c) shows that $-\langle W \rangle$ and η qualitatively peak at $\phi_{W'} = 2.05$ and $\phi_{\eta} = 2.53$, respectively. In the small- ϕ regime ($\phi < \phi_{W'}$), the difference between Δp_4 and Δp_3 is enhanced as the increase of ϕ is attempting to raise $|1 - 2\zeta|$ [Fig. 3(d)]. However, in the large- ϕ regime ($\phi > \phi_{W'}$), the decrease of the discrepancy $\gamma - \delta$ determines the reduction of $\Delta p_4 - \Delta p_3$. In addition, $-\langle W \rangle$ and $\Delta p_4 - \Delta p_3$ have a strongly positive, linear relationship. Overall, $\langle Q_M \rangle$ rapidly decreases with the growth of ϕ , since the increase of the transition probabilities δ and ζ with respect to increasing ϕ whittles down Δp_3 . The above analysis reveals that the engine under the finite-time unitary transformations

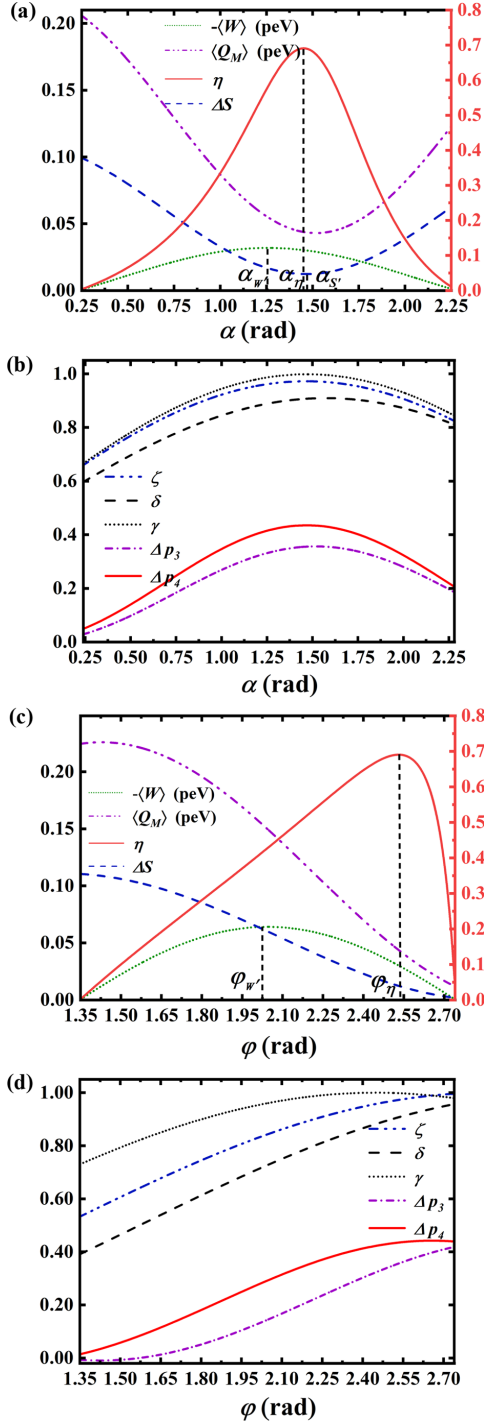


FIG. 3. Shown for a given value ϕ_η of ϕ are the curves of (a) the work output $-\langle W \rangle$, input energy $\langle Q_M \rangle$, efficiency η , and entropy change during the measurement process ΔS and (b) the transition probabilities ζ , δ , and γ and the differences Δp_3 and Δp_4 in probability distributions between the ground and excited states varying with the colatitude α . Shown for a given value α_η of α are the curves of (c) the work output $-\langle W \rangle$, input energy $\langle Q_M \rangle$, efficiency η , and entropy change during the measurement process ΔS and (d) the transition probabilities ζ , δ , and γ and the differences Δp_3 and Δp_4 in probability distributions between the ground and excited states varying with the longitude ϕ . In (a) and (c) the left vertical axis shows values for $-\langle W \rangle$ and $\langle Q_M \rangle$, while the right vertical axis shows the corresponding scale of η .

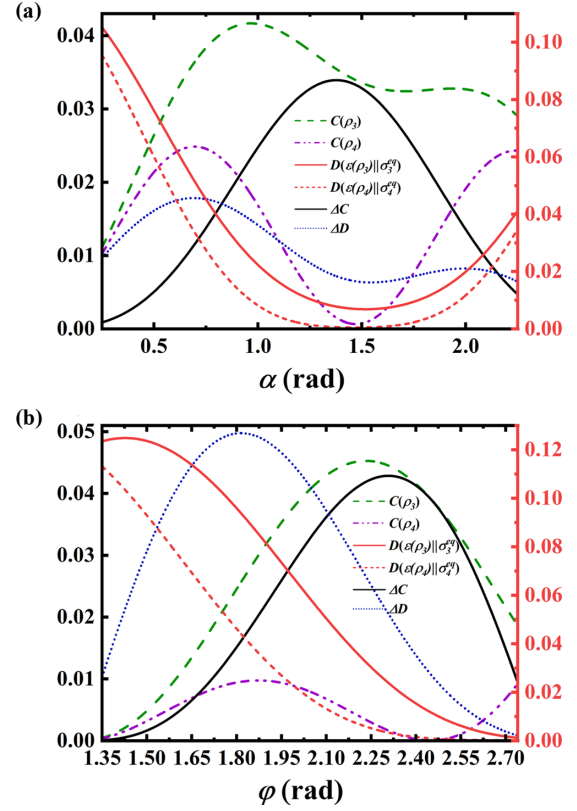


FIG. 4. Shown for a given value ϕ_η of ϕ are the curves of (a) the coherences $C(\rho_3)$ and $C(\rho_4)$ and their difference $\Delta C = C(\rho_3) - C(\rho_4)$ and the KLU divergences $D(\varepsilon(\rho_3)\|\sigma_3^{\text{eq}})$ and $D(\varepsilon(\rho_4)\|\sigma_4^{\text{eq}})$ and their difference $\Delta D = D(\varepsilon(\rho_3)\|\sigma_3^{\text{eq}}) - D(\varepsilon(\rho_4)\|\sigma_4^{\text{eq}})$ varying with the colatitude α . Shown for a given value α_η of α are the curves of (b) the coherences $C(\rho_3)$ and $C(\rho_4)$ and their difference $\Delta C = C(\rho_3) - C(\rho_4)$ and the KLU divergences $D(\varepsilon(\rho_3)\|\sigma_3^{\text{eq}})$ and $D(\varepsilon(\rho_4)\|\sigma_4^{\text{eq}})$ and their difference $\Delta D = D(\varepsilon(\rho_3)\|\sigma_3^{\text{eq}}) - D(\varepsilon(\rho_4)\|\sigma_4^{\text{eq}})$ varying with the longitude ϕ . In (a) and (b) the left vertical axis shows values for $C(\rho_3)$, $C(\rho_4)$, ΔC , and ΔD , while the right vertical axis shows the corresponding scales of $D(\varepsilon(\rho_3)\|\sigma_3^{\text{eq}})$ and $D(\varepsilon(\rho_4)\|\sigma_4^{\text{eq}})$. Here $C(\rho_2)$ and $D(\varepsilon(\rho_2)\|\sigma_2^{\text{eq}})$ remain constant at any given values of α and ϕ and are not shown on the graph.

realizes the work extraction without changing the spin transition frequency. It should be pointed out that this result was obtained in Ref. [43], where a coherent rotation around the y axis of the Bloch sphere in the unitary transformation strokes is considered. The angles of the measurement basis on the Bloch sphere determine the upper limits on the average work output and efficiency. Again, Fig. 3(c) also shows that the maximum value for the efficiency is found for small values of entropy change during the measurement process.

Finally, we would like to show how the angles of the measurement basis circumvent the degradation effect of the coherence on the performance. Therefore, the coherence of a given state ρ_i is expressed as the entropy difference $C(\rho_i) = S[\varepsilon(\rho_i)] - S(\rho_i)$ [19–21,67], where $\varepsilon(\rho_i) = \sum_k |k\rangle\langle k|\rho_i|k\rangle\langle k|$ is a full dephasing map of ρ_i in the reference basis with respect to the instantaneous eigenstate $|k\rangle$ of the Hamiltonian H_i (note that $H_3 = H_2$ and $H_4 = H_1$). For a standard Otto cycle, coherences generated in the adiabatic expansion and compression

processes are associated with entropy production and quantum friction. However, when the thermalization is incomplete, Camati *et al.* adopted the definition of $C(\rho_i)$ and demonstrated that the careful tuning of cycle parameters makes coherence act like a dynamical quantum lubricant [19]. For the current cycle driven by quantum measurement, the work output and the input energy (see [64]) are written in terms of $C(\rho_i)$, i.e.,

$$-\langle W \rangle = \frac{1}{\beta} [C(\rho_3) + D(\varepsilon(\rho_3) \parallel \sigma_3^{\text{eq}}) - C(\rho_4) - D(\varepsilon(\rho_4) \parallel \sigma_4^{\text{eq}}) - C(\rho_2) - D(\varepsilon(\rho_2) \parallel \sigma_2^{\text{eq}})] \quad (8)$$

and

$$\langle Q_M \rangle = \frac{1}{\beta} [C(\rho_3) + D(\varepsilon(\rho_3) \parallel \sigma_3^{\text{eq}}) - C(\rho_2) - D(\varepsilon(\rho_2) \parallel \sigma_2^{\text{eq}}) + \Delta S], \quad (9)$$

with $D(\varepsilon(\rho_i) \parallel \sigma_i^{\text{eq}}) = \text{Tr}\{\varepsilon(\rho_i)[\ln \varepsilon(\rho_i) - \ln \sigma_i^{\text{eq}}]\}$ defining the Kullback-Leibler-Umegaki (KLU) divergence between states $\varepsilon(\rho_i)$ and σ_i^{eq} and $\sigma_i^{\text{eq}} = e^{-\beta H_i} / \text{Tr}(e^{-\beta H_i})$ describing the Gibbs state that is in thermal equilibrium contact with the bath at inverse temperature β . As $\Delta S > 0$ [Fig. 2(c)], the efficiency has the potential to be enhanced by reducing $\langle Q_M \rangle$ through the decrease of ΔS . It is seen clearly from Eqs. (8) and (9) that suppressing the coherence $C(\rho_4)$ of state ρ_4 , i.e., decreasing $C(\rho_4)$, can significantly improve both the work output and the efficiency. It is observed in Figs. 3 and 4 that the position of the minimum $C(\rho_4)$ is quite close to that of maximum efficiency. Figure 4 further indicates that $\Delta C = C(\rho_3) - C(\rho_4)$ does not change monotonically with $C(\rho_3)$ or $C(\rho_4)$ and $\Delta D = D(\varepsilon(\rho_3) \parallel \sigma_3^{\text{eq}}) - D(\varepsilon(\rho_4) \parallel \sigma_4^{\text{eq}})$ does not change monotonically with $D(\varepsilon(\rho_3) \parallel \sigma_3^{\text{eq}})$ or $D(\varepsilon(\rho_4) \parallel \sigma_4^{\text{eq}})$, because the coherences $C(\rho_3)$ and $C(\rho_4)$ [the divergences $D(\varepsilon(\rho_3) \parallel \sigma_3^{\text{eq}})$ and $D(\varepsilon(\rho_4) \parallel \sigma_4^{\text{eq}})$] are not independent of each other. Thus, the work output and the efficiency form complex relationships with $C(\rho_3)$, since they are simultaneously affected by $D(\varepsilon(\rho_3) \parallel \sigma_3^{\text{eq}})$. However, it is

significant to note that although the state of the maximum ΔC does not correspond to that of the maximum work output or the maximum efficiency, it is located in the optimal range between the maximum work output and the maximum efficiency, as illustrated in Figs. 3 and 4.

V. CONCLUSION

Recent advances have shown the possibility of harnessing the energy provided by quantum measurements. We have developed here a measurement-based single-qubit quantum engine and shown how quantum measurement is able to work as a fuel in a quantum cycle. The present model employs a Hamiltonian that does not commute at different times, thus generating coherence in the energy basis of the working substance and then decreasing the performance of the quantum engine. By assuming sufficient control under the measurement basis angles α and φ , we are able to circumvent the degradation effect due to coherence and increase the extracted work and efficiency. Thus, a suitable choice of the measurement basis effectively works as a kind of quantum lubrication, since it suppresses the effect of the coherence produced in stage III.

Our results indicate that quantum measurement can be useful to build quantum thermodynamic cycles beyond the standard ones with two thermal baths. In addition, the numerical simulation considers parameters usually employed in NMR, which opens the possibility to experimentally test the measurement-based single-qubit quantum engine. We hope that this work can help reveal the role played by measurement in quantum thermodynamics and its applications.

ACKNOWLEDGMENTS

This work was supported by the National Natural Science Foundation of China (Grants No. 11805159 and No. 12075197) and the Natural Science Foundation of Fujian Province (Grant No. 2019J05003). J.F.G.S. acknowledges São Paulo Research Grant No. 2019/04184-5.

-
- [1] J. Roßnagel, S. T. Dawkins, K. N. Tolazzi, O. Abah, E. Lutz, F. Schmidt-Kaler, and K. Singer, A single-atom heat engine, *Science* **352**, 325 (2016).
 - [2] R. Kosloff, Quantum thermodynamics: A dynamical viewpoint, *Entropy* **15**, 2100 (2013).
 - [3] B. Lin and J. Chen, Performance analysis of an irreversible quantum heat engine working with harmonic oscillators, *Phys. Rev. E* **67**, 046105 (2003).
 - [4] J. He, J. Chen, and B. Hua, Quantum refrigeration cycles using spin- $\frac{1}{2}$ systems as the working substance, *Phys. Rev. E* **65**, 036145 (2002).
 - [5] T. B. Batalhão, A. M. Souza, L. Mazzola, R. Auccaise, R. S. Sarthour, I. S. Oliveira, J. Goold, G. De Chiara, M. Paternostro, and R. M. Serra, Experimental Reconstruction of Work Distribution and Study of Fluctuation Relations in a Closed Quantum System, *Phys. Rev. Lett.* **113**, 140601 (2014).
 - [6] J. Åberg, Fully Quantum Fluctuation Theorems, *Phys. Rev. X* **8**, 011019 (2018).
 - [7] K. Micadei, G. T. Landi, and E. Lutz, Quantum Fluctuation Theorems Beyond Two-Point Measurements, *Phys. Rev. Lett.* **124**, 090602 (2020).
 - [8] A. M. Timpanaro, G. Guarnieri, J. Goold, and G. T. Landi, Thermodynamic Uncertainty Relations from Exchange Fluctuation Theorems, *Phys. Rev. Lett.* **123**, 090604 (2019).
 - [9] S. Lee, M. Ha, and H. Jeong, Quantumness and thermodynamic uncertainty relation of the finite-time Otto cycle, *Phys. Rev. E* **103**, 022136 (2021).
 - [10] M. F. Sacchi, Thermodynamic uncertainty relations for bosonic Otto engines, *Phys. Rev. E* **103**, 012111 (2021).
 - [11] Y. Zhang, Optimization performance of quantum Otto heat engines and refrigerators with squeezed thermal reservoirs, *Physica A* **559**, 125083 (2020).
 - [12] X. L. Huang, T. Wang, and X. X. Yi, Effects of reservoir squeezing on quantum systems and work extraction, *Phys. Rev. E* **86**, 051105 (2012).

- [13] M. O. Scully, M. S. Zubairy, G. S. Agarwal, and H. Walther, Extracting work from a single heat bath via vanishing quantum coherence, *Science* **299**, 862 (2003).
- [14] F. L. S. Rodrigues, G. De Chiara, M. Paternostro, and G. T. Landi, Thermodynamics of Weakly Coherent Collisional Models, *Phys. Rev. Lett.* **123**, 140601 (2019).
- [15] J. D. Cresser and J. Anders, Weak and Ultrastrong Coupling Limits of the Quantum Mean Force Gibbs State, *Phys. Rev. Lett.* **127**, 250601 (2021).
- [16] P. Strasberg, G. Schaller, N. Lambert, and T. Brandes, Nonequilibrium thermodynamics in the strong coupling and non-Markovian regime based on a reaction coordinate mapping, *New J. Phys.* **18**, 073007 (2016).
- [17] H. P. Breuer, E.-M. Laine, and J. Piilo, Measure for the Degree of Non-Markovian Behavior of Quantum Processes in Open Systems, *Phys. Rev. Lett.* **103**, 210401 (2009).
- [18] E.-M. Laine, J. Piilo, and H.-P. Breuer, Measure for the non-Markovianity of quantum processes, *Phys. Rev. A* **81**, 062115 (2010).
- [19] P. A. Camati, J. F. G. Santos, and R. M. Serra, Coherence effects in the performance of the quantum Otto heat engine, *Phys. Rev. A* **99**, 062103 (2019).
- [20] J. P. Santos, L. C. Céleri, G. T. Landi, and M. Paternostro, The role of quantum coherence in non-equilibrium entropy production, *npj Quantum Inf.* **5**, 23 (2019).
- [21] G. Francica, J. Goold, and F. Plastina, Role of coherence in the nonequilibrium thermodynamics of quantum systems, *Phys. Rev. E* **99**, 042105 (2019).
- [22] A. M. Zagoskin, S. Savel'ev, Franco Nori, and F. V. Kusmartsev, Squeezing as the source of inefficiency in the quantum Otto cycle, *Phys. Rev. B* **86**, 014501 (2012).
- [23] P. Abiuso and V. Giovannetti, Non-Markov enhancement of maximum power for quantum thermal machines, *Phys. Rev. A* **99**, 052106 (2019).
- [24] Y. Shirai, K. Hashimoto, R. Tezuka, C. Uchiyama, and N. Hatano, Non-Markovian effect on quantum Otto engine: Role of system-reservoir interaction, *Phys. Rev. Res.* **3**, 023078 (2021).
- [25] G. Guarnieri, C. Uchiyama, and B. Vacchini, Energy backflow and non-Markovian dynamics, *Phys. Rev. A* **93**, 012118 (2016).
- [26] P. A. Camati, J. F. G. Santos, and R. M. Serra, Employing non-Markovian effects to improve the performance of a quantum Otto refrigerator, *Phys. Rev. A* **102**, 012217 (2020).
- [27] A. Pozas-Kerstjens, E. G. Brown, and K. V. Hovhannisyann, A quantum Otto engine with finite heat baths: Energy, correlations, and degradation, *New J. Phys.* **20**, 043034 (2018).
- [28] R. J. de Assis, J. S. Sales, J. A. R. da Cunha, and N. G. de Almeida, Universal two-level quantum Otto machine under a squeezed reservoir, *Phys. Rev. E* **102**, 052131 (2020).
- [29] J. Klaers, S. Faelt, A. Imamoglu, and E. Togan, Squeezed Thermal Reservoirs as a Resource for a Nanomechanical Engine beyond the Carnot Limit, *Phys. Rev. X* **7**, 031044 (2017).
- [30] J. Roßnagel, O. Abah, F. Schmidt-Kaler, K. Singer, and E. Lutz, Nanoscale Heat Engine Beyond the Carnot Limit, *Phys. Rev. Lett.* **112**, 030602 (2014).
- [31] J. P. S. Peterson, T. B. Batalhão, M. Herrera, A. M. Souza, R. S. Sarthour, I. S. Oliveira, and R. M. Serra, Experimental Characterization of a Spin Quantum Heat Engine, *Phys. Rev. Lett.* **123**, 240601 (2019).
- [32] J. Klatzow, J. N. Becker, P. M. Ledingham, C. Weinzetl, K. T. Kaczmarek, D. J. Saunders, J. Nunn, I. A. Walmsley, R. Uzdin, and E. Poem, Experimental Demonstration of Quantum Effects in the Operation of Microscopic Heat Engines, *Phys. Rev. Lett.* **122**, 110601 (2019).
- [33] T. Denzler, J. F. G. Santos, E. Lutz, and R. M. Serra, Nonequilibrium fluctuations of a quantum heat engine, *arXiv:2104.13427*.
- [34] L. Szilard, Über die entropieverminderung in einem thermodynamischen system bei eingriffen intelligenter wesen, *Z. Phys.* **53**, 840 (1929).
- [35] H. S. Leff and A. F. Rex, *Maxwell's Demon: Entropy, Information, Computation, Computing* (Princeton University Press, Princeton, 1990).
- [36] C. Elouard, D. Herrera-Martí, B. Huard, and A. Auffèves, Extracting Work from Quantum Measurement in Maxwell's Demon Engines, *Phys. Rev. Lett.* **118**, 260603 (2017).
- [37] J. J. Park, K.-H. Kim, T. Sagawa, and S. W. Kim, Heat Engine Driven by Purely Quantum Information, *Phys. Rev. Lett.* **111**, 230402 (2013).
- [38] S. Toyabe, T. Sagawa, M. Ueda, E. Muneyuki, and M. Sano, Information heat engine: Converting information to energy by feedback control, *Nat. Phys.* **6**, 988 (2010).
- [39] J. Yi, P. Talkner, and Y. W. Kim, Single-temperature quantum engine without feedback control, *Phys. Rev. E* **96**, 022108 (2017).
- [40] X. Ding, J. Yi, Y. W. Kim, and P. Talkner, Measurement driven single temperature engine, *Phys. Rev. E* **98**, 042122 (2018).
- [41] C. Elouard and A. N. Jordan, Efficient Quantum Measurement Engines, *Phys. Rev. Lett.* **120**, 260601 (2018).
- [42] K. Brandner, M. Bauer, M. T. Schmid, and U. Seifert, Coherence-enhanced efficiency of feedback-driven quantum engines, *New J. Phys.* **17**, 065006 (2015).
- [43] A. N. Jordan, C. Elouard, and A. Auffèves, Quantum measurement engines and their relevance for quantum interpretations, *Quantum Stud.: Math. Found.* **7**, 203 (2020).
- [44] L. Buffoni, A. Solfanelli, P. Verrucchi, A. Cuccoli, and M. Campisi, Quantum Measurement Cooling, *Phys. Rev. Lett.* **122**, 070603 (2019).
- [45] L. Bresque, P. A. Camati, S. Rogers, K. Murch, A. N. Jordan, and A. Auffèves, Two-Qubit Engine Fueled by Entanglement and Local Measurements, *Phys. Rev. Lett.* **126**, 120605 (2021).
- [46] Y. Aharonov, D. Z. Albert, and L. Vaidman, How the Result of a Measurement of a Component of the Spin of a Spin- $\frac{1}{2}$ Particle Can Turn Out to be 100, *Phys. Rev. Lett.* **60**, 1351 (1988).
- [47] I. M. Duck, P. M. Stevenson, and E. C. G. Sudarshan, The sense in which a "weak measurement" of a spin- $\frac{1}{2}$ particle's spin component yields a value 100, *Phys. Rev. D* **40**, 2112 (1989).
- [48] R. Flack and B. J. Hiley, Weak measurement and its experimental realisation, *J. Phys.: Conf. Ser.* **504**, 012016 (2014).
- [49] D. Ueda, H. Ohta, and S. Yokoo, Revisiting weak measurement in light of thermodynamics, *arXiv:1910.12189*.
- [50] S. K. Manikandan, C. Elouard, K. W. Murch, A. Auffèves, and A. N. Jordan, Efficiently fuelling a quantum engine with incompatible measurements, *arXiv:2107.13234*.
- [51] O. Hosten and P. Kwiat, Observation of the spin hall effect of light via weak measurements, *Science* **319**, 787 (2008).

- [52] J. S. Lundeen, B. Sutherland, A. Patel, C. Stewart, and C. Bamber, Direct measurement of the quantum wavefunction, *Nature (London)* **474**, 188 (2011).
- [53] J. T. Monroe, N. Y. Halpern, T. Lee, and K. W. Murch, Weak Measurement of a Superconducting Qubit Reconciles Incompatible Operators, *Phys. Rev. Lett.* **126**, 100403 (2021).
- [54] K. Jacobs, *Quantum Measurements Theory and its Applications* (Cambridge University Press, Cambridge, 2014).
- [55] H. M. Wiseman and G. J. Milburn, *Quantum Measurement and Control* (Cambridge University Press, Cambridge, 2010).
- [56] Y. Rezek, Reflections on friction in quantum mechanics, *Entropy* **12**, 1885 (2010).
- [57] T. Feldmann and R. Kosloff, Quantum lubrication: Suppression of friction in a first-principles four-stroke heat engine, *Phys. Rev. E* **73**, 025107(R) (2006).
- [58] R. Kosloff and T. Feldmann, Discrete four-stroke quantum heat engine exploring the origin of friction, *Phys. Rev. E* **65**, 055102(R) (2002).
- [59] I. S. Oliveira, T. J. Bonagamba, R. S. Sarthour, J. C. C. Freitas, and E. R. deAzevedo, *NMR Quantum Information Processing* (Elsevier, Amsterdam, 2007).
- [60] H. T. Quan, Y. Liu, C. P. Sun, and F. Nori, Quantum thermodynamic cycles and quantum heat engines, *Phys. Rev. E* **76**, 031105 (2007).
- [61] J. Chen, H. Dong, and C. Sun, Bose-Fermi duality in a quantum Otto heat engine with trapped repulsive bosons, *Phys. Rev. E* **98**, 062119 (2018).
- [62] G. Manzano, F. Plastina, and R. Zambrini, Optimal Work Extraction and Thermodynamics of Quantum Measurements and Correlations, *Phys. Rev. Lett.* **121**, 120602 (2018).
- [63] S. Lloyd, Quantum-mechanical Maxwell's demon, *Phys. Rev. A* **56**, 3374 (1997).
- [64] See Supplemental Material at <http://link.aps.org/supplemental/10.1103/PhysRevA.104.062210> for further details.
- [65] M. Campisi, P. Hänggi, and P. Talkner, Colloquium: Quantum fluctuation relations: Foundations and applications, *Rev. Mod. Phys.* **83**, 771 (2011).
- [66] J. Ehrich, M. Esposito, F. Barra, and J. M. R. Parrondo, Microreversibility and thermalization with collisional baths, *Physica A* **552**, 122108 (2020).
- [67] G. Francica, F. C. Binder, G. Guarnieri, M. T. Mitchison, J. Goold, and F. Plastina, Quantum Coherence and Ergotropy, *Phys. Rev. Lett.* **125**, 180603 (2020).